crystallization communications

Crystallization and preliminary crystallographic studies of *Mycobacterium tuberculosis* DNA gyrase B C-terminal domain, part of the enzyme reaction core

Guangsen Fu,[a,b] **Jinjun Wu,**[b,c] **Deyu Zhu,**[a,b] **Yonglin Hu,**[a] **Lijun Bi,**[a] **Xian-En Zhang**[c] **and Da-Cheng Wang**[a]*

[a]National Laboratory of Biomacromolecules, Institute of Biophysics, Chinese Academy of Sciences, Beijing 100101, People's Republic of China, [b]Graduate University of Chinese Academy of Sciences, Beijing 100039, People's Republic of China, and [c]State Key Laboratory of Virology, Wuhan Institute of Virology, Chinese Academy of Sciences, Wuhan 430071, People's Republic of China

Correspondence e-mail: dcwang@ibp.ac.cn

DNA gyrase subunit B C-terminal domain (GyrB-CTD) is a functional module of DNA gyrase which participates in forming the core of DNA gyrase and plays critical roles in G-segment binding and T-segment loading and passage. Here, the purification, crystallization and preliminary X-ray crystallographic studies of GyrB-CTD from *Mycobacterium tuberculosis* H37Rv are reported. Diffraction data were collected from crystals of native GyrB-CTD and its selenomethionine derivative to resolutions of 2.8 and 3.0 Å, respectively. These crystals belonged to space group $P2_12_12_1$ with similar unit-cell parameters. The native protein crystals had unit-cell parameters $a = 52.831$, $b = 52.763$, $c = 192.579$ Å.

1. Introduction

DNA gyrase is a type IIA topoisomerase that introduces supercoils into DNA (Wang, 1996). It is an intriguing molecular machine that catalyzes the ATP-dependent transport of one DNA segment (the T-segment) through a transient break in another segment (the G-segment) to directly modulate DNA topology (Champoux, 2001). It is critical for the survival of cellular organisms and is also an important target of antibacterial drugs (Heddle & Maxwell, 2002). The molecular architecture of the prokaryotic gyrase exists in the form (GyrA)$_2$(GyrB)$_2$, which is distinct from the homodimers (ATPase-B′-A′)$_2$ of the eukaryotic type II topoisomerases (Corbett & Berger, 2004). Both subunits, GyrA and GyrB, are generally composed of two domains: the N-terminal domain (NTD) and the C-terminal domain (CTD) (Lynn *et al.*, 1986). The GyrB-CTD and GyrA-NTD are from two separate polypeptides and cooperatively form the enzyme core, whereas the GyrB-NTD functions as an ATPase and the GyrA-CTD is involved in T-segment formation (Brino *et al.*, 2000).

Structural and functional studies on type II topoisomerases have established a 'two-gate' mechanism for the type IIA topoisomerases (Berger *et al.*, 1996). It is believed that DNA gyrase generally uses this mechanism for enzyme reaction (Costenaro *et al.*, 2007). In this scheme, the T-segment enters the enzyme through the molecular gate (the N-gate) formed by the dimeric ATPase domains on one side of the enzyme (GyrB-NTD) and exits through the GyrA-NTD carboxy-terminal dimerization interface (the C-gate). Passage of the T-segment through the cleaved G-segment is carried out on the third dimeric interface, termed the DNA-gate (Dong & Berger, 2007), in the GyrA-NTD. In addition, the T-segment is formed by the GyrA-CTD to wrap the proximal stretch of DNA (Corbett *et al.*, 2004). Evidently, navigation of the T-segment captured by the N-gate of the ATPase domain to the DNA-gate is a basic link in this mechanism scheme (Nöllmann *et al.*, 2007).

To date, the structural basis and possible mechanism of T-segment navigation are unknown. The GyrB-CTD is located between the N-gate and the DNA-gate as part of the enzyme reaction core, which suggests an important role of the GyrB-CTD in T-segment manipulation (Nöllmann *et al.*, 2007). A series of crystal structures of gyrase modules have been solved to date, including those of GyrB-NTD
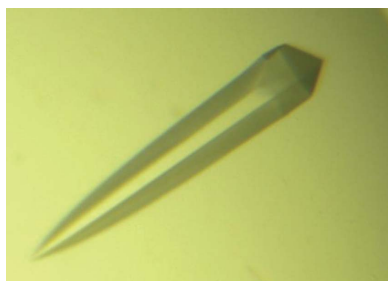
(ATPase), GyrA-NTD and GyrA-CTD (Brino *et al.*, 2000; Corbett *et al.*, 2004; Morais Cabral *et al.*, 1997), but that of GyrB-CTD has not yet been reported. The crystal structure determination of GyrB-CTD, which has been anticipated for a long time, will provide a comprehensive understanding of its functional roles and will shed light on the enzymatic mechanism, especially the T-segment navigation.

GyrB-CTD is also a major target of quinolone antibacterials (Heddle & Maxwell, 2002) and its structure would also contribute to structure-based quinolone-resistance research and novel antibacterial drug design. Here, we report the recombinant protein expression, purification and crystallization of GyrB-CTD, from which a solid foundation is set up for the future structural determination of this protein.

2. Materials and methods
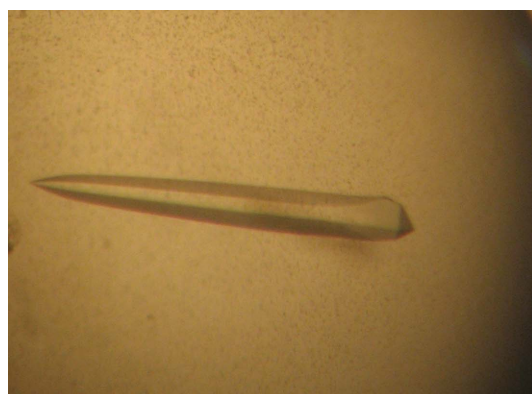
2.1. Cloning, expression and purification

The gene for the C-terminal domain containing residues 485–714 of *Mycobacterium tuberculosis* H37Rv GyrB was amplified from the expression plasmid pET32a-*gyrB* (Huang *et al.*, 2006). The native DNA GyrB-CTD gene was cloned into an expression vector derived from pET-20b(+) plasmid and was placed between *Nde*I and *Hin*dIII restriction sites. A six-histidine tag was engineered into the C-terminus of the GyrB-CTD protein, which resulted in an expressed protein with a molecular weight of 27.4 kDa. The plasmid was

(*a*)

Figure 1   (*b*)
(*a*) A crystal of native GyrB-CTD protein. (*b*) A crystal of SeMet GyrB-CTD protein

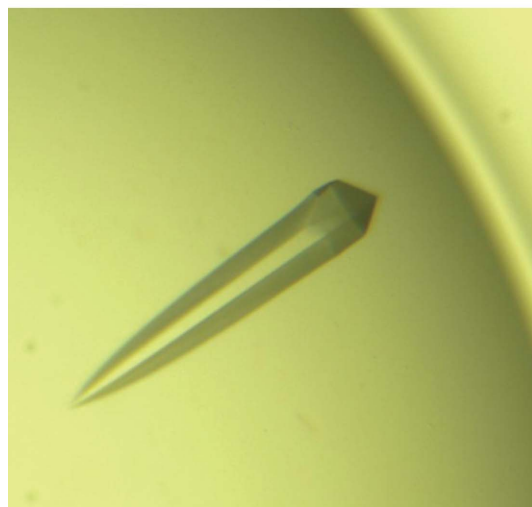amplified in TG1-competent *Escherichia coli* cells. The construct was confirmed by sequencing.

The recombinant plasmid was transformed into *E. coli* host strain BL21(DE3) pLysS competent cells. The transformed bacteria were grown on an LB plate containing ampicillin (100 µg ml^{-1}) and chloramphenicol (30 µg ml^{-1}) overnight at 310 K. A single colony was picked to inoculate 5 ml LB medium and cultured overnight. 1.5 ml of overnight culture was transferred into 50 ml fresh LB and incubation was continued for 3 h; 30 ml of the 50 ml bacterial culture was then transferred into 1 l fresh LB medium. All LB media used contained ampicillin (100 µg ml^{-1}) and chloramphenicol (30 µg ml^{-1}). The cells were induced with 0.5 mM isopropyl β-D-1-thiogalacto-pyranoside (IPTG) when the culture reached an OD$_{600}$ of 0.6–0.8. After induction, cultivation was continued for 5 h at 295 K. The cells were harvested by centrifugation at 6000g at 277 K for 15 min. The bacteria obtained were stored at 253 K for subsequent use. The purification was completed using an Ni–NTA affinity column (Novagen) and an ÄKTA purification system (Amersham Pharmacia). The cell pellet was resuspended in 30 ml lysis buffer (20 mM Tris–HCl pH 8.0, 500 mM NaCl, 10 mM imidazole) with 0.1 mM PMSF and the cells were lysed by ultrasonication. The lysate was centrifuged at 24 000g at 277 K for 40 min. The supernatant was loaded directly onto an Ni–NTA column (Novagen) which was pre-equilibrated with lysis buffer. The column was washed with wash buffer (20 mM Tris–HCl pH 8.0, 500 mM NaCl, 20 mM imidazole). GyrB-CTD containing a His$_6$ tag at its C-terminus was eluted with elution buffer (20 mM Tris–HCl pH 8.0, 500 mM NaCl, 250 mM imidazole). All steps of Ni–NTA affinity chromatography were performed at 277 K. The eluate was concentrated by ultrafiltration (Millipore) at 277 K and loaded onto a Superdex 75 HiLoad 16/60 column (Amersham Pharmacia) pre-equilibrated with 50 mM Tris–HCl pH 8.0, 400 mM NaCl at 289 K. The column flow rate was 1 ml min^{-1} and all peak fractions were collected. All fractions were identified by SDS–PAGE. Dimeric GyrB-CTD eluted at 54 ml. The peak was collected and supplemented with three volumes of 50 mM Tris–HCl pH 8.0 and the protein was then concentrated prior to crystallization. The selenomethionine-substituted (SeMet) derivative was produced by expression in the *E. coli met*$^{-}$ auxotrophic strain B834(DE3). The transformed B834(DE3) cells were grown in LB medium at 310 K. When the OD$_{600}$ of the culture reached 0.6–0.8, the cells were harvested and resuspended in minimal medium. After 90 min of culturing the cells under starvation, 50 mg selenomethionine was added per litre of culture. After a further 30 min, expression was induced as in the case of native protein. The purification of the SeMet protein was performed using the same method as that for the native protein.

2.2. Crystallization

The native and SeMet-derivative proteins were concentrated to approximately 5 mg ml^{-1}. Protein concentrations were determined from the absorbance at 280 nm, assuming an A_{280} of 0.673 for a 1.0 mg ml^{-1} solution. Initial crystallization screening for the native protein used Crystal Screen and Crystal Screen 2 from Hampton Research (Jancarik & Kim, 1991). The crystallization experiments were conducted using the hanging-drop vapour-diffusion method at 293 K (McPherson, 1999), with 2 µl drops containing 1 µl 5 mg ml^{-1} protein solution and 1 µl reservoir solution equilibrated over 0.5 ml reservoir solution. The crystallization conditions were optimized at 293 and 277 K by varying the type and concentration of precipitants (PEGs), the pH, the types of additives and the protein concentration.
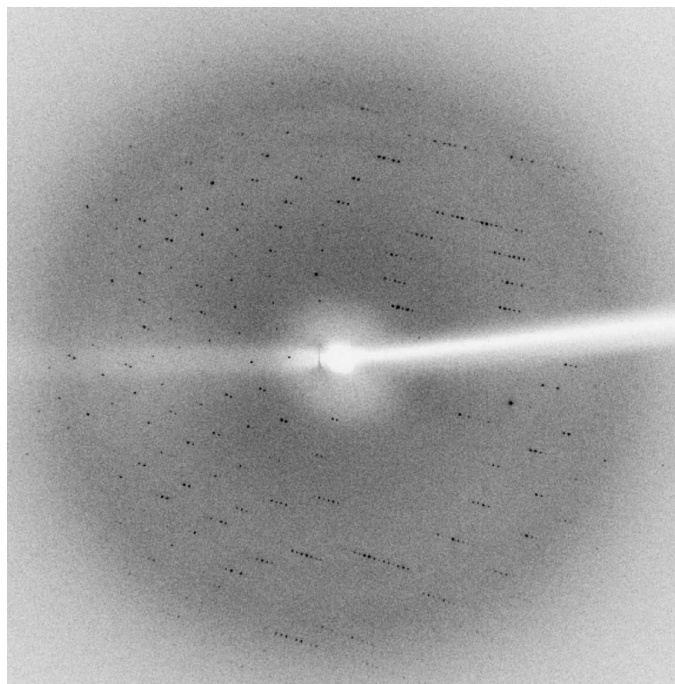
Figure 2
Native GyrB-CTD diffraction pattern image. The crystal diffracted to 2.8 Å resolution.

2.3. Data collection and processing

Two data sets were collected: one at the peak wavelength of 0.97947 Å from selenomethionine-substituted crystals on beamline BL5A, Photon Factory, KEK (Tsukuba, Japan) and the other at Cu $K\alpha$ radiation wavelength ($\lambda = 1.5418$ Å) using a Rigaku R-AXIS IV^{++} image-plate system mounted on a rotating-anode X-ray source operating at 40 kV and 20 mA with 0.1 mm confocal incident-beam diameter at the National Laboratory of Biomacromolecules, Institute of Biophysics, Chinese Academy of Sciences. *MOSFLM* (v.6.2.2; Leslie, 1992) and *SCALA* from the *CCP*4 program suite (v.4.2.2; Collaborative Computational Project, Number 4, 1994) were used for the processing, reduction and scaling of the diffraction data.

3. Results

In the initial screening, tiny single native crystals were observed in Crystal Screen conditions No. 41 [25%(*w/v*) PEG 3350, 0.1 *M* sodium acetate trihydrate pH 4.5] and No. 66 [25%(*w/v*) PEG 3350, 0.2 *M* ammonium sulfate, 0.1 *M* bis-tris pH 5.5] after 2 d. As the result of optimization, well shaped crystals (0.8 × 0.06 × 0.06 mm; 0.3 × 0.05 × 0.05 mm for the SeMet protein) of GyrB-CTD were obtained using hanging-drop vapour diffusion by mixing equal volumes of protein solution and reservoir solution containing 15–25% PEG 3350, 50 m*M* sodium acetate pH 4.5–5.0, 0.1–0.2 *M* ammonium sulfate (with an additional 5 m*M* DTT and 0.2 m*M* EDTA for the SeMet protein) and equilibrating over 0.5 ml reservoir solution at 277 K for about a week (Fig. 1). Prior to data collection, GyrB-CTD crystals were transferred to cryoprotectant solution containing 15% ethylene glycol, 15% PEG 3350, 50 m*M* sodium acetate pH 4.7–5.0, 0.2 *M* ammonium acetate and soaked for about 2 min; they were then immediately flash-frozen in a liquid-nitrogen stream on cryoloops.

Table 1
Statistics of X-ray data sets of native and SeMet GyrB-CTD crystals.

Values in parentheses are for the highest resolution shell.

Data set	Native	SeMet (peak)
Space group	$P2_12_12_1$	$P2_12_12_1$
Unit-cell parameters (Å, °)	$a = 52.831$, $b = 52.763$, $c = 192.579$, $\alpha = \beta = \gamma = 90$	$a = 52.770$, $b = 52.757$, $c = 192.662$, $\alpha = \beta = \gamma = 90$
Resolution (Å)	40.6–2.8 (2.95–2.8)	40.6–3.0 (3.16–3.0)
Wavelength (Å)	1.5418	0.97947
Unique reflections	13423	11442
Completeness (%)	96.3 (88.4)	100.0 (98.6)
Redundancy	5.7 (5.8)	13.7 (14.0)
Average $I/\sigma(I)$	9.5 (2.2)	5.6 (2.0)
R_{merge}† (%)	4.9 (34.8)	9.6 (37.3)

† $R_{merge} = \sum_{hkl} \sum_i |I_i(hkl) - \langle I(hkl) \rangle| / \sum_{hkl} \sum_i I_i(hkl)$, where $\langle I(hkl) \rangle$ is the mean of the observations $I_i(hkl)$ of reflection hkl.

The data-collection statistics of native and SeMet-derivative crystals are shown in Table 1. The native crystal diffracted to 2.8 Å resolution (Fig. 2). The crystals proved to be orthorhombic ($P2_12_12_1$) and unit-cell parameters of the native crystal were $a = 52.831$, $b = 52.763$, $c = 192.579$ Å, $\alpha = \beta = \gamma = 90°$. These data are compatible with the presence of two molecules in the asymmetric unit and a solvent content of 48.79%. The SeMet-derivative crystal diffracted to a resolution of 3.0 Å and belonged to the same space group, with similar unit-cell parameters to those of the native crystal.

References

Berger, J. M., Gamblin, S. J., Harrison, S. C. & Wang, J. C. (1996). *Nature (London)*, **379**, 225–232.
Brino, L., Urzhumtsev, A., Mousli, M., Bronner, C., Mitschler, A., Oudet, P. & Moras, D. (2000). *J. Biol. Chem.* **275**, 9468–9575.
Champoux, J. J. (2001). *Annu. Rev. Biochem.* **70**, 369–413.
Collaborative Computational Project, Number 4 (1994). *Acta Cryst.* D**50**, 760–763.
Corbett, K. D. & Berger, J. M. (2004). *Annu. Rev. Biophys. Biomol. Struct.* **33**, 95–118.
Corbett, K. D., Shultzaberger, R. K. & Berger, J. M. (2004). *Proc. Natl Acad. Sci. USA*, **101**, 7293–7298.
Costenaro, L., Grossmann, J. G., Ebel, C. & Maxwell, A. (2007). *Structure*, **15**, 329–339.
Dong, K. C. & Berger, J. M. (2007). *Nature (London)*, **450**, 1201–1205.
Huang, Y.-Y., Deng, J.-Y., Gu, J., Zhang, Z.-P., Maxwell, A., Bi, L.-J., Chen, Y.-Y., Zhou, Y.-F., Yu, Z.-N. & Zhang, X.-E. (2006). *Nucleic Acids Res.* **34**, 5650–5659.
Heddle, J. & Maxwell, A. (2002). *Antimicrob. Agents Chemother.* **46**, 1805–1815.
Jancarik, J. & Kim, S.-H. (1991). *J. Appl. Cryst.* **24**, 409–411.
Leslie, A. G. W. (1992). *Jnt CCP4/ESF–EACBM Newsl. Protein Crystallogr.* **26**.
Lynn, R., Giaever, G., Swanberg, S. L. & Wang, J. C. (1986). *Science*, **233**, 647–649.
McPherson, A. (1999). *Crystallization of Biological Macromolecules.* New York: Cold Spring Harbor Laboratory Press.
Morais Cabral, J. H., Jackson, A. P., Smith, C. V., Shikotra, N., Maxwell, A. & Liddington, R. C. (1997). *Nature (London)*, **388**, 903–906.
Nöllmann, M., Crisona, N. J. & Arimondo, P. B. (2007). *Biochimie*, **89**, 490–499.
Wang, J. C. (1996). *Annu. Rev. Biochem.* **65**, 635–692.